AAS 22-728

INVESTIGATING SOLAR RADIATION PRESSURE MODELING FOR OPERATIONS IN NEAR RECTILINEAR HALO ORBIT

Clark P. Newman[*], Jacob R. Hollister[†], Diane C. Davis[‡], and Emily M. Zimovan-Spreen[§]

NASA's Gateway program will build a crew-tended station in an Earth-Moon Near Rectilinear Halo Orbit (NRHO). Deep space operations differ considerably from Low Earth Orbit (LEO) operations in the environmental modeling, orbit geometry, and propagation timespans in operations. The cislunar environment, as opposed to the LEO environment, lacks atmospheric drag and is simultaneously affected by the gravity of both the Earth and the Moon, and solar radiation pressure (SRP) has a significant effect. This paper investigates the impacts of various SRP models on prediction accuracy, attitude control accuracy, orbit determination performance, and computational burden.

INTRODUCTION

Gateway Mission

The Gateway will be the first long-term habitable outpost operating beyond low Earth orbit. It will support missions in cislunar space, to the lunar surface, and missions into heliocentric space.[1] The Gateway mission will start with the Power and Propulsion Element (PPE) and Habitability And Logistics Outpost (HALO) launching together as a comanifested payload on a heavy lift rocket. The Comanifested Vehicle (CMV) will spiral out from Earth orbit and enter NRHO. Subsequent visiting vehicles will arrive at the NRHO and integrate with the Gateway, and crewed missions will dock with Gateway as a staging point for sorties to the surface. As vehicles integrate with the Gateway, its configuration, mass properties, and thus its controllability are changed. Gateway will grow over time, increasing in mass and surface area without gaining additional control authority. Analyzing and understanding the physical behavior of a growing station in cislunar space is paramount to pre-launch mission design success.

Near Rectilinear Halo Orbit

Long term operations of an outpost in NRHO will be considerably different than in LEO. The Gateway will be placed in a southern L2 NRHO that exhibits a 9:2 resonance with the lunar synodic period. The Gateway will perform 9 revolutions in the same time that the Moon orbits Earth twice, for a period of approximately 6.5 days.[2,3] Along the baseline NRHO, long periods of low velocity measured with respect to the Moon are punctuated by low altitude (3,500 km), high velocity perilune

[*]Senior Systems Engineer, a.i. solutions, Inc.
[†]Senior Systems Engineer, a.i. solutions, Inc.
[‡]Principal Systems Engineer, a.i. solutions, Inc.
[§]Aerospace Engineer, NASA

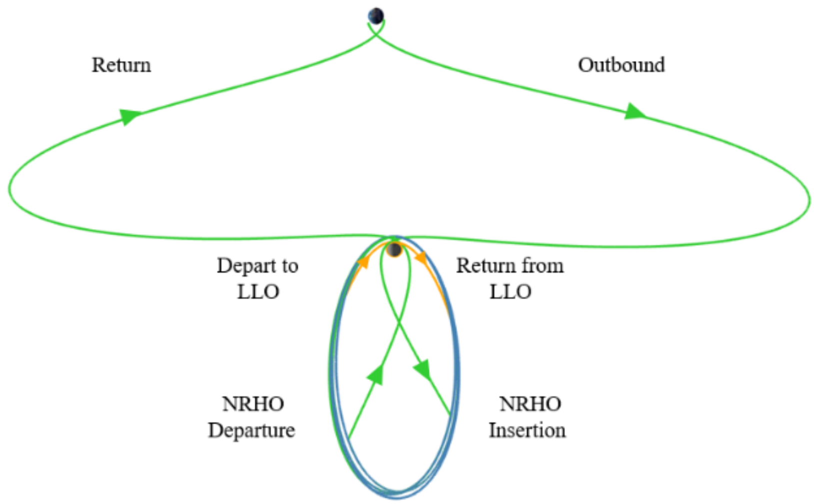

Figure 1: The NRHO in blue, surface excursions in orange, and direct transfers in green, as viewed in the Earth-Moon rotating frame.

passes that last on the order of hours. The baseline NRHO is an L2 halo orbit that is periodic in the Earth-Moon rotating frame and that is always visible from Earth. Note that due to this geometry, nearly all of the motion relative to the Earth is perpendicular to the range vector measured from the Earth to the Gateway.[5] The baseline NRHO's size and phasing allow a nearly eclipse-free trajectory for the 15 year lifetime of the mission.[4]

Solar Radiation Pressure

The Gateway will be perturbed by continuous SRP force, whose impact must be accounted for in mission design.[4] The current investigation addresses the fidelity of SRP force modeling in mission design and its impact on mission operations accuracy, performance, and speed.

When SRP forces are considered in simulation modeling, there is a spectrum of fidelity options available. A simple and effective model is the spherical model, whose solar radiation force is modeled as

$$\mathbf{F}_{\text{SRP}} = v\frac{S}{c}C_R A_S \left(\frac{\mathbf{r}_{\text{SC}}^{\odot}}{r_{\text{SC}}^{\odot}}\right) \tag{1}$$

where $\mathbf{F}_{\text{SRP}}$ is the SRP force, v is a binary shadow function (1 if in sunlight, 0 if in shadow), S is the solar constant at the range of the spacecraft to the Sun (typically 1367 $\frac{W}{m^2}$ at the distance of the Earth-Moon system from the Sun), c is the speed of light, C_R is the coefficient of reflectivity, A_S is the SRP area, and $\left(\frac{\mathbf{r}_{\text{SC}}^{\odot}}{r_{\text{SC}}^{\odot}}\right)$ is the unit vector from the Sun to the spacecraft. This formulation returns a force vector acting on the center of mass of the spacecraft, and is not suitable for analyzing torques generated by imbalanced SRP forces across the SRP area.

More complex SRP models consist of multiple flat plates with varying properties (e.g., coeffic- cient of diffuse reflectivity, surface area, etc.) arranged in the spacecraft body frame to bound the spacecraft geometry and emulate its reflective properties. The SRP force on a flat plate can be modeled as[6]

$$\mathbf{F}_{\text{SRP}} = -P_{\odot} S_i \left[2 \left(\frac{R^i_{\text{diff}}}{3} + R^i_{spec} \cos \theta^i_{\text{SRP}} \right) \mathbf{n}^i_B + \left(1 - R^i_{\text{spec}} \right) \mathbf{s} \right] \max \left(\cos \theta^i_{SRP}, 0 \right) \tag{2}$$

where $\mathbf{F}_{\text{SRP}}$ is the resultant SRP force on the i^{th} plate, $P_{\odot}$ is the SRP at a specific distance from the Sun, S_i is the area of the i^{th} plate, R^i_{diff} is the coefficient of diffuse reflectivity, R^i_{spec} is the coefficient of specular reflectivity, θ^i_{SRP} is the angle between the i^{th} plate and Sun direction, $\mathbf{n}^i_B$ is the unit normal of the i^{th}, and $\mathbf{s}$ is the unit vector from the plate center of pressure to the Sun. The forces of individual plates are summed to obtain the aggregate SRP force that perturbs the spacecraft. The spacecraft is torqued by[6]

$$\mathbf{L}_{\text{SRP}} = \sum_{i=0}^{N} \mathbf{r}^i \times \mathbf{F}^i_{\text{SRP}} \tag{3}$$

where $\mathbf{r}^i$ is the vector from the spacecraft center of mass to the center of pressure of the i^{th} plate. A flat plate model represents an increase in modeling fidelity as compared to the spherical model, with many more parameters to consider. Each modeled plate has a position, orientation, area, and three coefficients of reflectivity to consider. Additional plates will have unique spatial information and possibly unique reflective properties.

By increasing the number of plates considered, the fidelity of the flat plate model for SRP computations increases. However, an increase in fidelity requires a simulataneous increase the number of required computations for simulations. A nominal flat plate model does not consider self-shadowing, however ray-tracing methods, at the expense of additional computational burden, are one option to increase in fidelity. In time-sensitive operations, a trade off between performance and computational speed may be necessary to increase overall mission performance and robustness.

Legacy Mission Modeling

Various recent missions have included SRP in the mission design phase and operations of the spacecraft. The Lunar Reconnaissance Orbiter (LRO) was launched in June 2009 and operated in low lunar orbit before being positioned into a frozen orbit for long term storage. For the LRO mission development, a model of ten plates which comprised the spacecraft body, the solar panels, and two high gain antennas was considered for SRP modeling. However this model was not available until post-launch, so the flat plate model was only used in concert with laser range reprocessing. For Orbit Determination (OD) operations and product generation, a spherical model was employed. For the mission science phase, LRO received 30 minutes of tracking once per two-hour orbit period. In comparison, the propagation time between uncrewed Gateway passes will be about two days apart.[7]

The Mars Reconnaissance Orbiter (MRO) was launched in August 2005 and entered a low Martian orbit after a seven month cruise. The MRO is modeled as a nine-component structure, with their orientation defined with respect to the spacecraft frame. The attitude of the spacecraft is available through telemetry or predicted and generated. Combining the attitude with the component knowledge, the total SRP area can be calculated. The estimates for reflectivity coefficients are reconstructed during the OD process and updated during cruise. The MRO model does not consider torques generated by solar radiation pressure.[8]

Currently in pre-mission simulations for attitude control, the Gateway is modeled with flat plates, which can range from 14 plates for the first configuration to 112 plates for the largest configuration. Solar panels and body panels are given unique C_R values, but are not solved for directly in the Orbit Determination (OD) process. The sunlit panels produce an SRP force and torque about the center of mass. The SRP torque is included in momentum integration for attitude control simulation. Solar panels are rotated on their pivot axis to be perpendicular to solar rays, while radiator panels are rotated to be parallel to solar rays. No high gain antennas are considered as flat plates in the model.

NRHO OPERATIONS

NRHO Operations are generally repeated over the 6.5 day period, with occasional unique mission events. These events include Rendezvous and Proximity Operations (RPOD) when Visiting Vehicles (VVs) arrive or depart, Extra-Vehicular Activities (EVAs) while Orion is present, slews to targets of interest, and transfers to different cislunar trajectories.

A typical uncrewed NRHO with some operational events called out is shown in Figure 2. There are three DSN two-way tracking data passes every NRHO revolution. The first pass ends 24 hours before targeting the Orbit Maintenance Maneuver (OMM), which is then executed at true anomaly $\nu = 200°$. The second pass starts 24 hours before perilune, and the third pass ends 24 hours after perilune. Each pass is eight hours long. The tick marks on the NRHO are roughly 25 hours apart.

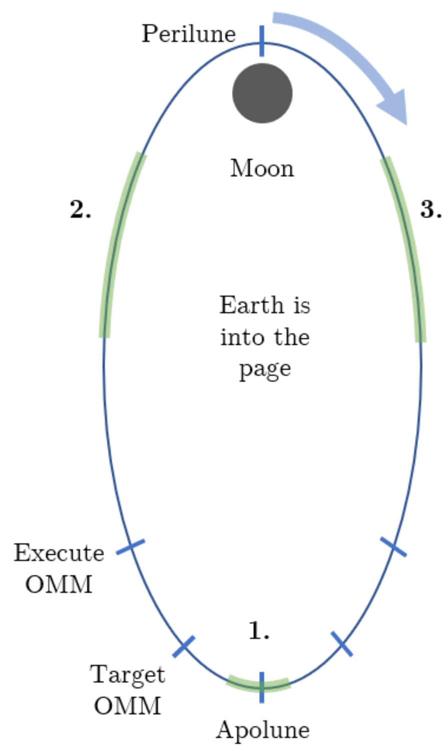

Figure 2: Simplified representation of common operations in the NRHO. Data arcs are in green and numbered.

While the Gateway is uncrewed, it is assumed that the Gateway will be constantly tracked by DSN 2-way range and range-rate. Orion will perform a powered flyby and then insert into the NRHO and dock before apolune, as seein in Figure 1. From a pre-perilune location along the NRHO, the Human Lander System (HLS) undocks and depart to LLO then trasitions down to the lunar surface. After a single revolution in the NRHO, the HLS will depart LLO and return to the NRHO to dock with the Gateway post-perilune. Along this revolution, a nominal data cutoff exists 24 hours before OMM targeting, which is executed 48 hours after data cutoff. While the Gateway is crewed, there are periodic venting forces and torques, along with forces and torques from desaturation maneuvers to remove the system momentum and maintain attitude orientation. For any crewed analysis it is assumed there is a wastewater vent approximately every six hours, which in turn triggers a desaturation maneuver.

Table 1: Simulated Error Sources

Parameter Name	1-σ uncertainty	Notes
Initial Position Error	10 km	
Initial Velocity Error	1 cm/s	
Relative Mass Error	30%	
Relative SRP Area Error	30%	
Desaturation Maneuver ΔV	3.33 mm/s	1, 2
Uncrewed OMM Constant Error	0.47 mm/s	
Uncrewed OMM Magnitude Error	0.5%	
Crewed OMM Magnitude Error	0.5%	
OMM Pointing Error	0.333°	

[1] Desaturation occurs once before OMM execution and three times at perilune for both uncrewed and crewed configurations.
[2] Crewed configurations every 6 hours.

Table 2: Tracking Data Quality Parameters

Parameter	Value (1-σ)
Range Noise (m)	1.0
Range Bias (m)	7.5
Range Rate Noise (mm/s)	0.1

Other Modeling and Error Sources

In addition to SRP, venting, and desaturation maneuvers, the Gateway is subject to perturbations and mismodelings that further stress accuracy in predictions and OD. The lunar gravity is modeled with spherical harmonics of 24 $\times$ 24 order and degree, while in the OD filter, the estimated spacecraft is propagated with a 12 $\times$ 12 order and degree lunar spherical harmonics model. The complex Moment of Inertia (MOI) tensor is calculated for every Gateway configuration and utilized to consider lunar gravity gradient torques on the vehicle, which can trigger desaturation maneuvers that reduce system angular momentum and impart a small velocity perturbation. Tables 1 and 2 contain a summary of error sources and tracking data error and noise magnitudes used in the simulations.

Solar Pressure Equilibrium Attitude

The Gateway structure can be asymmetrical and has solar panels extending from the Power and Propulsion Element (PPE) which is situated at one end of the vehicle. The SRP acting on the sunlit surfaces of the Gateway will produce a force and torque on the vehicle that will perturb its velocity and induce rotation. The rotation will be arrested by Reaction Wheel Assemblies (RWAs), that transfer the imparted angular momentum into the RWAs to maintain a particular attitude. Eventually the RWAs will achieve their maximum rotation rate and will need to be "desaturated" with a maneuver that trades momentum from the RWAs with torque generated by thrusters to despin the RWAs while maintaining attitude. These desaturation maneuvers expend propellant and impart a small random velocity perturbation.

For longevity of the propellant budget and reduction of velocity perturbations, the Gateway will maintain a Solar Pressure Equilibrium Attitude (SPEA) that minimizes the total SRP torque experienced by the vehicle. This attitude balances the torques from SRP on sunlit surfaces about the vehicle center of mass. Generally, every Gateway configuration has two SPEAs: one where the center of SRP is directly between the center of mass and the Sun, and one where it is in line with the Sun and beyond the center of mass. The SPEA where the center of SRP is behind the center of mass is considered stable as deviations from that attitude will produce torques that tend to return the vehicle to SPEA. Below in Figure 3 is a depiction of a Gateway configuration in SPEA with the flat plates shaded according to the magnitude of SRP force imparted on them. The main solar panels

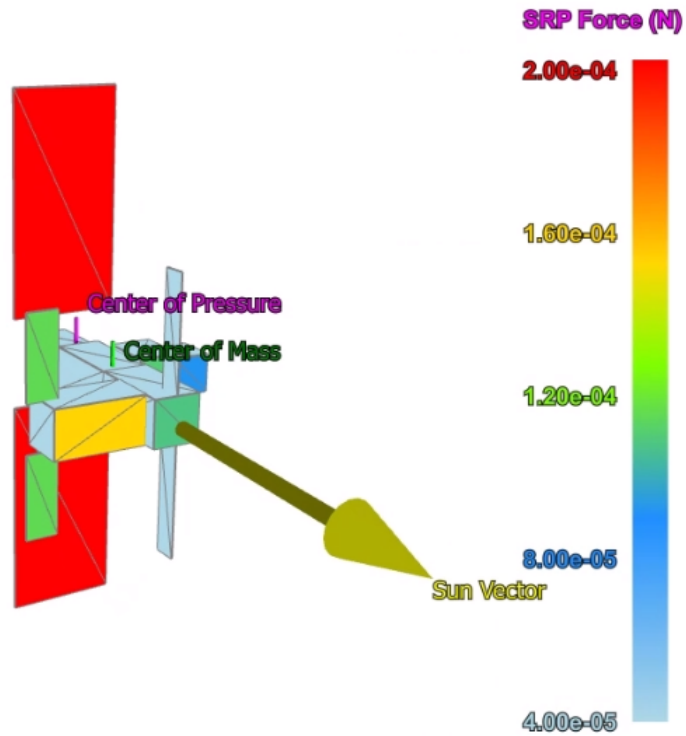

Figure 3: A visual representation of the baseline flat plate model with plates shaded by the SRP force magnitude imparted on them.

align with the Gateway body frame Z axis, and are the main drivers of SRP force imparted on the Gateway. The center of mass and center of pressure of this configuration are labeled showing the center of mass between the center of pressure and the Sun along the Gateway body X axis, which makes this a stable SPEA. This configuration has a mass of approximately 39,000 kg, and total solar panel of approximately 345 m^2.

SPEA is calculated for each Gateway configuration using a flat plate model and a differential corrector. That attitude is then held for nominal propagation through the NRHO. When the configuration changes from a docking or undocking event, the mass properties and SRP area properties change, and SPEA is recalculated.

Orbit Maintenance Maneuvers

Once per revolution, an orbit maintenance maneuver is targeted at twenty-four hours before its execution location at true anomaly $\nu = 200°$. Targeted maneuvers below 3.0 cm/s are waived. It has been shown that waiving maneuvers below this magnitude does not affect total ΔV budget while it reduces the total number of maneuver events. Uncrewed OMMs are executed with Solar Electric Propulstion (SEP) fueled by xenon, and crewed OMMs are executed with RCS thrusters fueled by hydrazine.

OMMs are targeted with a differential corrector using a receding horizon algorithm. The spacecraft V_X in the Earth-Moon rotating frame is targeted from the execution epoch to an epoch at perilune over six revolutions into the future. The differential corrector solves a maneuver which reduces the error between this velocity and the V_X at the corresponding perilune passage along in the reference trajectory. To maintain eclipse-free phasing, the epoch of the downstream perilune passage is targeted against the reference, using the solution from targeting V_X as the initial guess.[?]

To execute an OMM, the Gateway performs a yaw-roll-yaw sequence of rotations to achieve the burn direction attitude from SPEA while avoiding sunlight on particular faces of Gateway components. While crewed, the final yaw rotation to the burn attitude is executed with RCS thrusters, which expends propellant and slightly perturbs the velocity. Otherwise slews are executed with the RWAs; RWA slews require a longer duration than RCS slews. Thus, an uncrewed OMM, including the slews from and to SPEA, can take up to three hours of time away from SPEA and changes the solar forces on the spacecraft.

Configuration Changes

The Gateway will be integrated over time reminiscent of the integration of the International Space Station (ISS) at a smaller scale and around a different central body. Additional elements will arrive as visiting vehicles and directly dock to their configuration location or arrive combined with an Orion spacecraft as a co-manifested vehicle. The Human Lander System (HLS) will also depart for a surface excursion, and only the ascent element will return. All of these configuration change the total mass, the center of mass, and the center of SRP.

Docking events occur closer to apolune to avoid the highly-sensitive dynamics of perilune. Direct transfers can use a powered flyby of the Moon to intercept the NRHO close to apolune. Ballistic transfers of uncrewed vehicles take much longer in transit but are able to rendezvous the NRHO at any location and with low relative velocities. A docking or undocking event induces velocity perturbations from plume and contact forces.

Configuration changes will significantly alter the mass properties and SRP flat plate modeling, which in turn affects SPEA, slew rates, OMM burn times, and the magnitude of perturbations from desaturation maneuvers and venting events.

PROPAGATION COMPARISONS

SRP acts on Sunlit surfaces of a spacecraft and causes forces and torques on the craft that depend on its orientation, geometry, and surface material optical properties. The forces and torques that result from SRP can be included in simulation modeling or ignored, depending on the mission environment, tracking data scenario, and mission requirements. For missions in LEO, atmospheric drag is typically the dominating external force on a spacecraft, with perturbations from SRP forces being "in the noise" with respect to available tracking data. Without an atmosphere to consider for spacecraft in the NRHO, SRP forces are a primary driver of trajectory perturbations. SRP forces will act on the Gateway at all times, and spacecraft state predictions to perilune are important to spacecraft operations, so the fidelity of SRP modeling in simulating predictions to perilune will affect the accuracy of those predictions, at the cost of computational burden.

To investigate the trade-off between computational speed and prediction accuracy, a comparison simulation was developed in FreeFlyer. Starting from an eclipse-free NRHO reference trajectory, a spacecraft with a flat plate model that bounds a notional Gateway is treated as a baseline spacecraft that is propagated in SPEA through time in the NRHO for several revolutions. Comparison spacecraft with both spherical and flat plate models are propagated through the same time span and compared to the baseline spacecraft. The baseline spacecraft is a notional Gateway configuration that includes multiple attached components for increased complexity, and is depicted in Figure 3.

Compared against the baseline spacecraft with flat plate model in SPEA are multiple spherical models of various SRP area and a flat plate model held at spacecraft X-axis pointed toward the Sun. In Figures 4(a) and 4(b), the errors between SRP models and the baseline are shown for one day and the total comparison span, respectively. The top plots are position error over time in meters, and the bottom plots depict velocity errors in mm/s. Note that the total span plots in Figure 4(b) are in log scale along the Y axis.

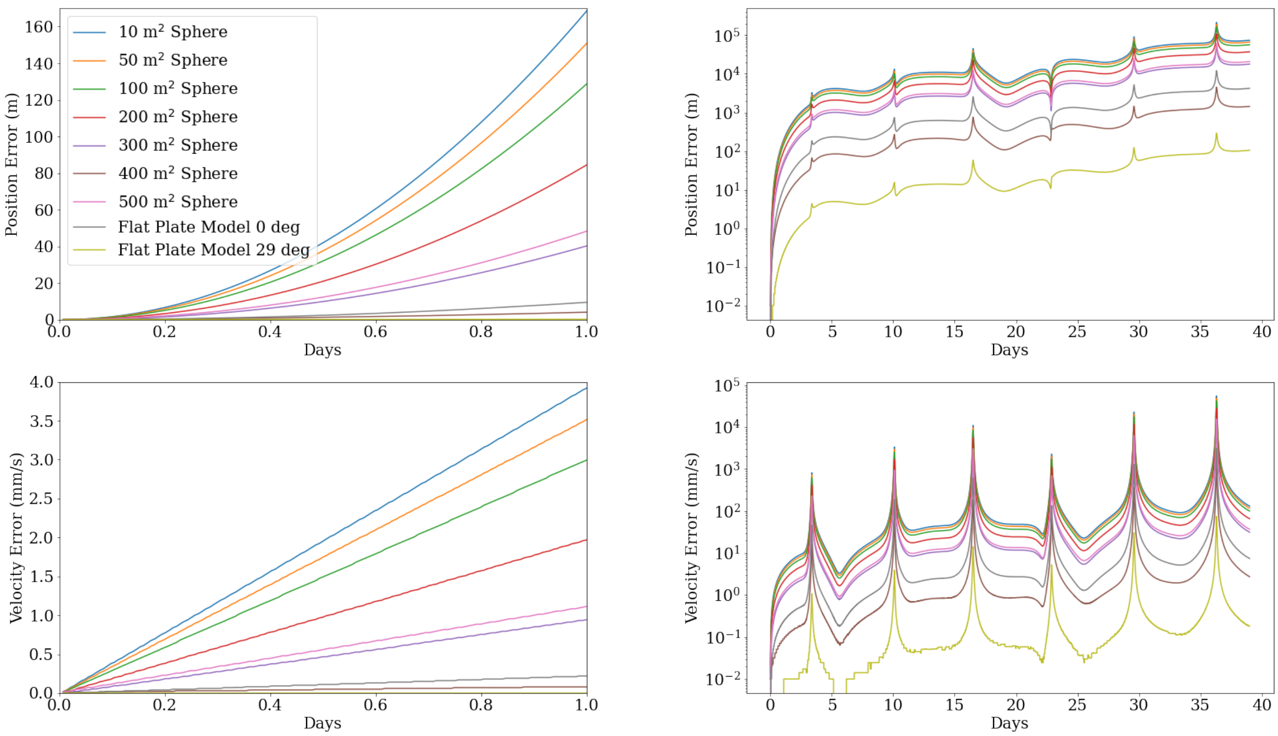

(a) First Day

(b) Total Span

Figure 4: Propagation Comparisons of various SRP models against the baseline flat plate model at 30 $^\circ$ yaw.

The 10 m^2 sphere performs the worst in comparison to the baseline over the first day, with an error of 160 meters. In contrast, as the spherical models increase in area to more closely approximate the nominal flat plate model of Gateway at SPEA, the errors decrease. This trend of decreasing error ends with the 500-m^2 spherical SRP model, whose error is larger than the 400-m^2 spherical model. The flat plate model at zero degrees yaw (body X-axis is pointing toward the Sun) has larger error than the 400-m^2 spherical model. The flat plate model at 29 degrees yaw (one degree of attitude error) lies on top of the X-axis. In the total span plots of Figure 4(b), the flat plate model with one degree of attitude error performs better than the rest of the models. However the flat plate model at zero degrees yaw performs worse than the 400-m^2 sphere. This suggests that while a flat plate model can be more accurate than a spherical model, attitude errors within the model can create propagation errors that exceed that of an appropriately-sized spherical model.

There is a computational cost to the additional considerations of a flat plate model. The simulations and comparisons were run under a scripting profiler which counts the number of instances a particular line of code is executed and also the amount of time spent on each line of code. For all of the comparisons, the nominal spacecraft with a flat plate model is propagated in a loop with the comparison spacecraft. This allows the profiler to directly compare execution time between the nominal and test case models. Absolute machine time will vary, but the nominal flat plate model required 2.6 times more computation time to propagate than the spherical model. These results suggest two operational considerations: the flat plate model may be more accurate than a spherical model if the correct attitude information is taken into account, but will consistently be approximately 2.6 times slower than the spherical model. Accurate knowledge of attitude is required to out-perform a spherical model.

To investigate a more concise comparison between the models, another comparison simulation is run. The flat plate model of the baseline Gateway at SPEA returns a SRP area that is then applied to a spherical model. The spherical model with the consistent SRP area is then compared against the baseline alongside flat plate models of varying yaw angle. In Figures 5(a) and 5(b), the position and velocity errors of the flat plate model at various yaw angle errors as well as a spherical model of area equal to the flat plate model at SPEA are plotted against the baseline flat plate model at SPEA. The SRP area of the flat plate model simply assigned to the spherical model is insufficient to capture the underlying dynamics, as it is the worst performing model.

ORBIT DETERMINATION

In LEO operations, the ballistic coefficient or some equivalent measure of drag property is often estimated in the course of OD operations. An accurate estimate of the ballistic coefficient improves navigation filter state estimates and predictions from state estimates. Similarly in deep space, an accurate estimate of the coefficient of reflectivity (C_R) or equivalent measure of SRP property can improve state estimates and predictions.[9] There are significant differences, naturally, in the behavior of drag as compared to SRP. For example, drag always acts in the anti-velocity direction while SRP acts in the Sun-spacecraft direction. The geometry of OD in LEO versus the NRHO is significantly different. This paper analyzes OD performance in estimating the coefficient of reflectivity under different tracking scenarios and compares the OD performance between simulations of increasing SRP modeling fidelity.

An OD simulation is run to investigate the ramifications of flat plate modeling inside the OD process. In this simulation, the truth spacecraft has a flat plate SRP model, which in turn is estimated with a spherical model. The simulation is run for the first two NRHO revolutions in a Monte Carlo process subject to the pertubations of the initial C_R estimate and random Deep Space Network (DSN) biases. If C_R is observable, the filter is expected to converge to a consistent value that may be offset from a spherical model. The biased estimated C_R may more closely reflect the actual SRP area and be the value that returns the best predictive accuracy performance. In Figure 6, the estimated C_R errors are shown in blue, with the positive and negative filter 1-σ values in red.

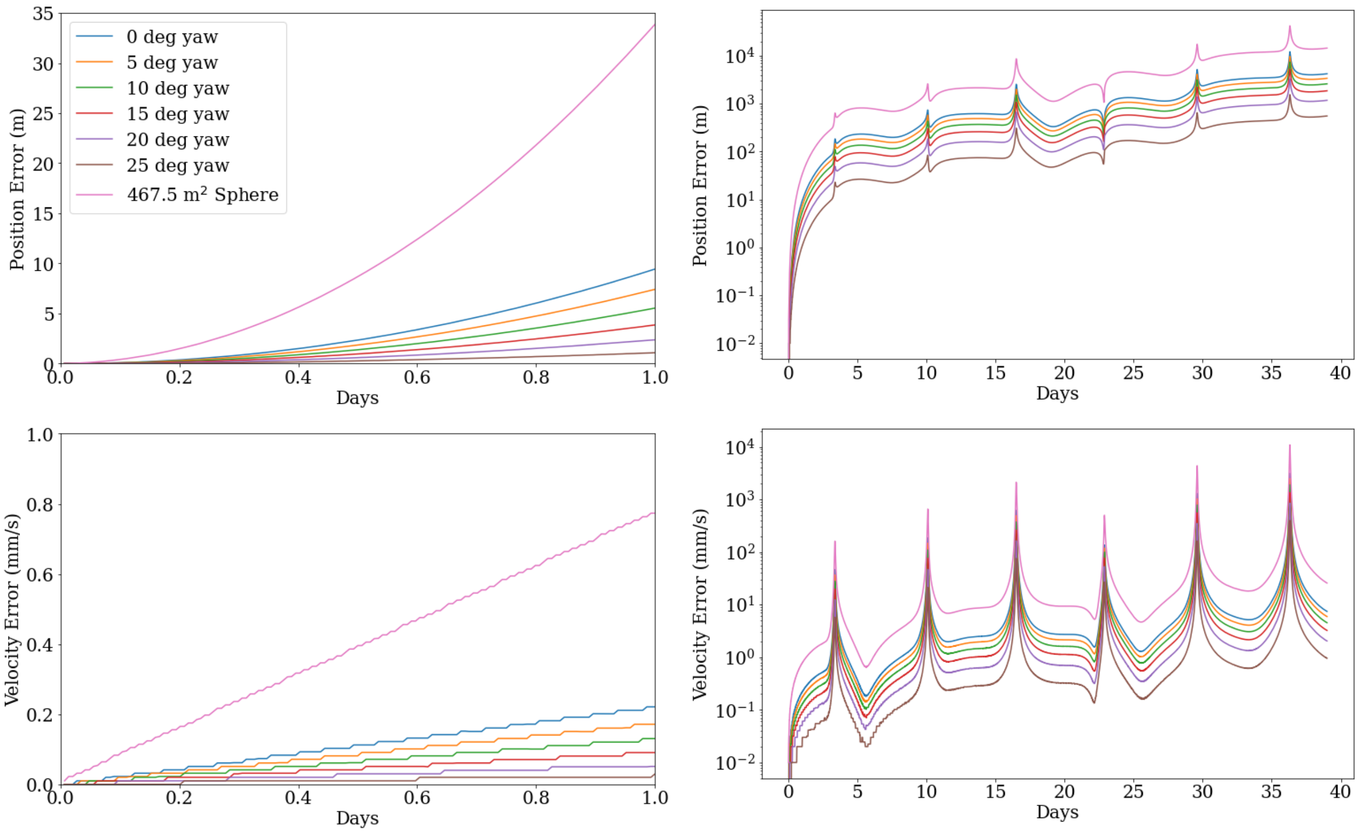

(a) First Day (b) Total Span

Figure 5: Propagation Comparisons of various SRP models against the baseline flat plate model in SPEA

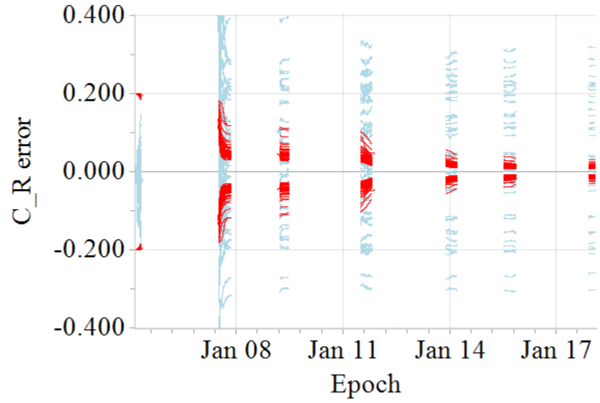

Figure 7: $\mathbf{C_R}$ estimate error (blue) and filter 1-σ values (red) of a spherical spacecraft estimating a flat plate model spacecraft in a Monte Carlo simulation. The truth area is perturbed to force the C_R estimate to unique values.

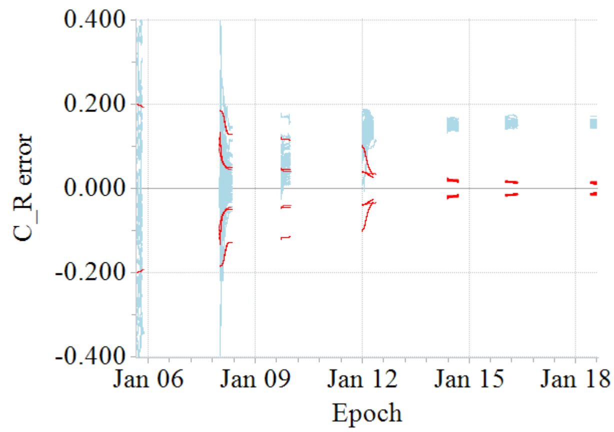

Figure 6: $\mathbf{C_R}$ estimate error (blue) and filter 1-σ values (red) of a spherical spacecraft estimating a flat plate model spacecraft in a Monte Carlo simulation

Figure 6 shows that the filter consistently converges to an estimated C_R error of approximately 0.16. The true C_R is 1.0, so the estimated C_R is 1.16. In this simulation of the first configuration, the estimated spherical SRP area is 330 m^2, but the truth flat plate model returns an SRP area of roughly 347 m^2, a ratio of 1.05. These area values are compared in a predictive accuracy analysis later on.

To further stress the filter and understand the behavior, the problem is rearranged so that the estimated SRP area is randomized instead of the C_R. In this case, the ratio of estimated SRP area and flat plate SRP area changes between Monte Carlo iterations, and the estimated C_R is expected to follow suit and at least move in the direction of the true SRP area to estimated SRP area ratio to unique values. Below in Figure 7, the estimated C_R errors are shown in blue, with the positive and negative filter 1-σ values in red, but here the initial estimated C_R begins consistently at 1.0 and it is the estimated SRP area that is randomized. The filter converges to a unique C_R in each Monte Carlo iteration with reduced σ, showing that the filter is able to nominally estimate SRP area in the NRHO using sparse DSN 2-way tracking.

Finally, a predictive comparison is performed between the flat plate model and spheres of 330 m^2, 347 m^2, and $1.16 * (\text{SRP Area})|_{\text{est}} = 383$ m^2. This is to test if the estimated spherical SRP area

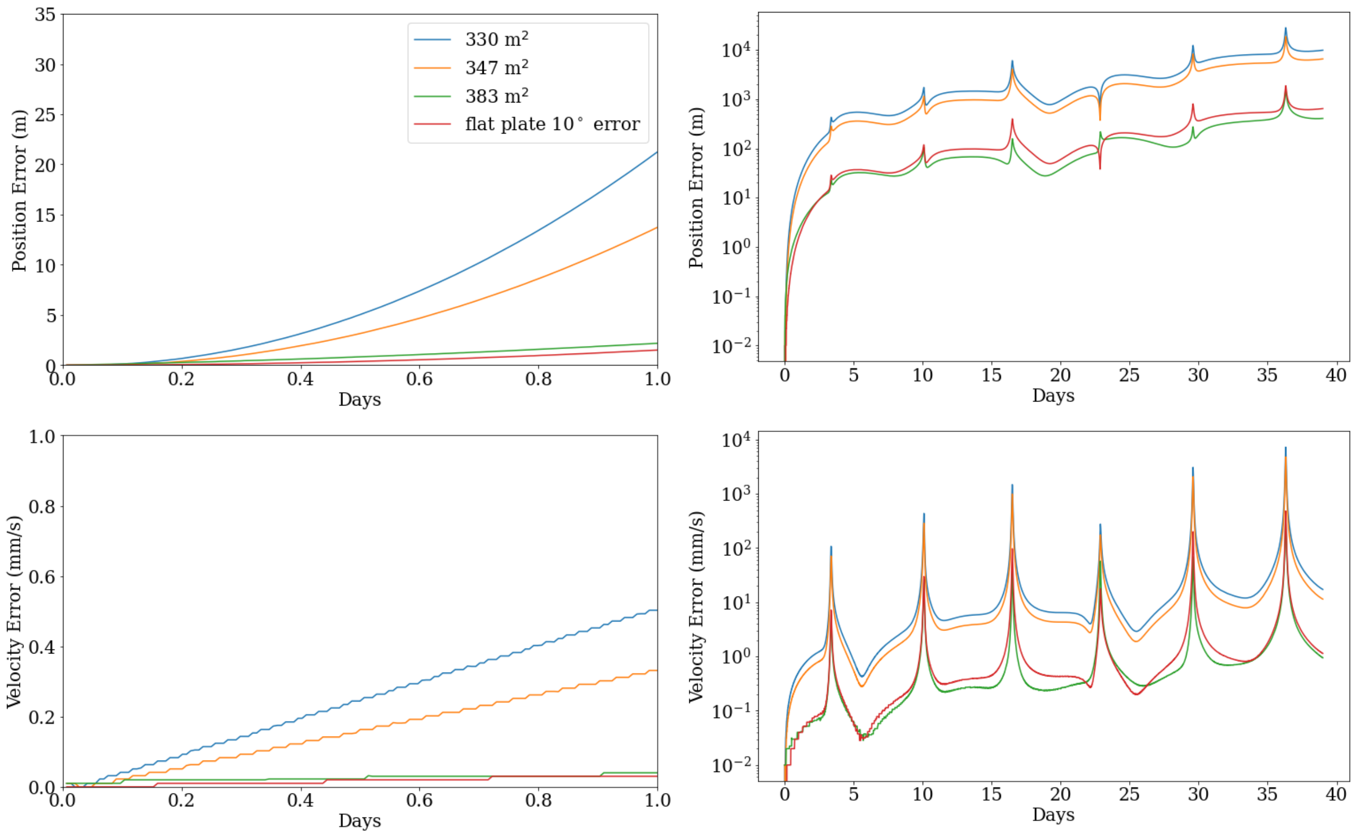

(a) First Day

(b) Total Span

Figure 8: Propagation Comparisons of the initial estimated SRP Area (blue), the flat plate area on a sphere (orange), the filter estimated SRP area equivalent (green), and a flat plate model with 10° yaw error.

equivalent model performs better than the flat plate model area cast to a sphere. In Figures 8(a) and 8(b), a prediction comparison is shown for the first day and for six revolutions in the left and right columns, respectively, with position errors in the top row and velocity errors in the bottom row.

The 383 m^2 sphere predicts with considerably smaller errors against the flat plate model as compared to a sphere of equal area to the flat plate model and the initial estimate of the vehicle SRP area. The 383 m^2 sphere prediction error magnitudes closely follow that of a flat plate model with 10° of attitude error in the yaw direction. These results show that it is possible to estimate a flat plate model in the NRHO with a sphere so that the predictive accuracy using that sphere is comparable to the predictive accuracy from estimating a flat plate model. One can reasonably model their estimated spacecraft (in this particular NRHO and with this specific tracking data) as a sphere when in reality the spacecraft is far from spherical.

ATTITUDE CONTROL

The Gateway is perturbed by SRP forces and rotated by SRP torques. The Gateway will be three-axis stabilized in a Solar Pressure Equilibrium Attitude (SPEA) to minimize SRP torques and maintain that attitude with minimal momentum buildup in the Reaction Wheel Assemblies

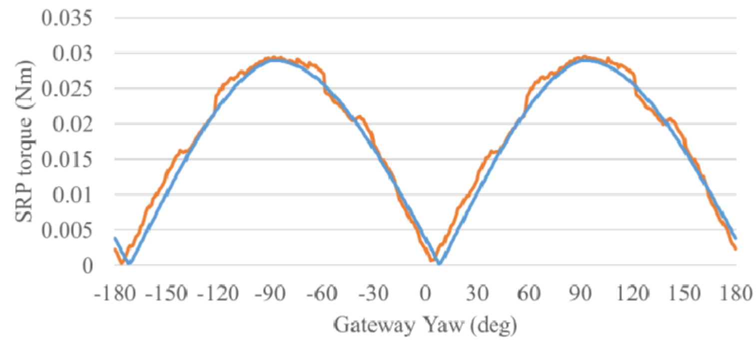

Figure 9: SRP Torque (Nm) vs Yaw Angle (deg) for a complex model (orange) and a simple model (blue)

(RWAs). Determining this attitude requires modeling the Gateway SRP behavior to some fidelity that is acceptable to the mission. In Figure 9, the SRP torque as a function of yaw angle is shown for a complex plate model in orange, and a simple model in blue.[10] The torque curves largely match except for small random deviations and a slight difference in the minimum torque yaw angles.

The deviations are from components that cause self-shadowing on another part of the Gateway vehicle either moving into or out of sunlight as the Gateway's yaw angle changes with respect to the Sun. The torque curves show that there are two SPEAs in each SRP model and that they vary from each other by approximately four degrees. It is shown previously in this paper that the predictive accuracy degrades with increasing attitude error. In a previous analysis,[10] a flat plate model was compared to a 3D Computer Assisted Design (CAD) model under a matrix of photon vectors. It is not feasible for the CAD model under a matrix of photon vectors to be modeled during long term simulations due to the computational burden. In response, the flat plate model is updated to include a measure of self-shadowing.

To include the effects of self-shadowing on the existing flat plate model, a similar approach is taken to apply a matrix of photon vectors to the flat plate model and identify the first intersecting surface. Applying the photon vector matrix method[9] to the flat plate model simplifies the underlying model from a 3D CAD model, which reduces the computational burden of a complex CAD model rotating in simulation space. Below in Figures 10(a) and 10(b) are visualizations of the flat plate model with sunlit points on it, and only the sunlit points, respectively.

The flat plate model is covered in "sun sensor" points which are polled for a particular attitude to determine if a direct line of sight to the Sun exists. The influence of self-shadowing is apparent in Figure 10(b) where a section of the radially docked element is missing several white points, which are unlit. The sun sensor points can be preconditioned by the flat plate model for which panels are pointed toward the Sun only to accelerate the processing of sunlit points. By placing the sun sensor points on the flat plate model, we also avoid the case where we are polling solar vectors that miss the Gateway entirely and do not return a sunlit or shadowed surface.

To investigate the impact of including self-shadowing in the torque model, the SRP torque magnitude is calculated for a matrix of solar-oriented attitudes. Starting from a direct Gateway body X-axis to Sun attitude, the SRP torque magnitude is calculated for different combinations of pitch and yaw variations from this attitude over a range of values for each. In Figure 11, a heatmap is displayed to visualize the SRP torques experienced over a range of plausible sun-oriented attitudes.

The highest torque experienced is above 0.012 Nm, which will saturate a 500 Nms capacity RWA

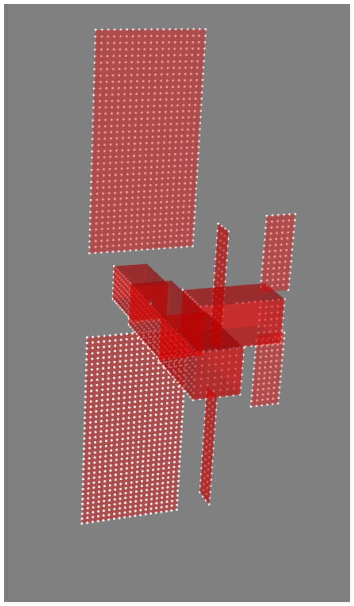

(a) Flat Plate Model with Sunlit Points

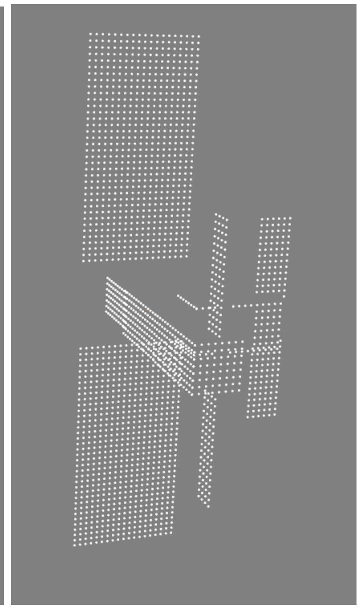

(b) Sunlit Points Only

Figure 10: Gateway flat plate model with self-shadow consideration.

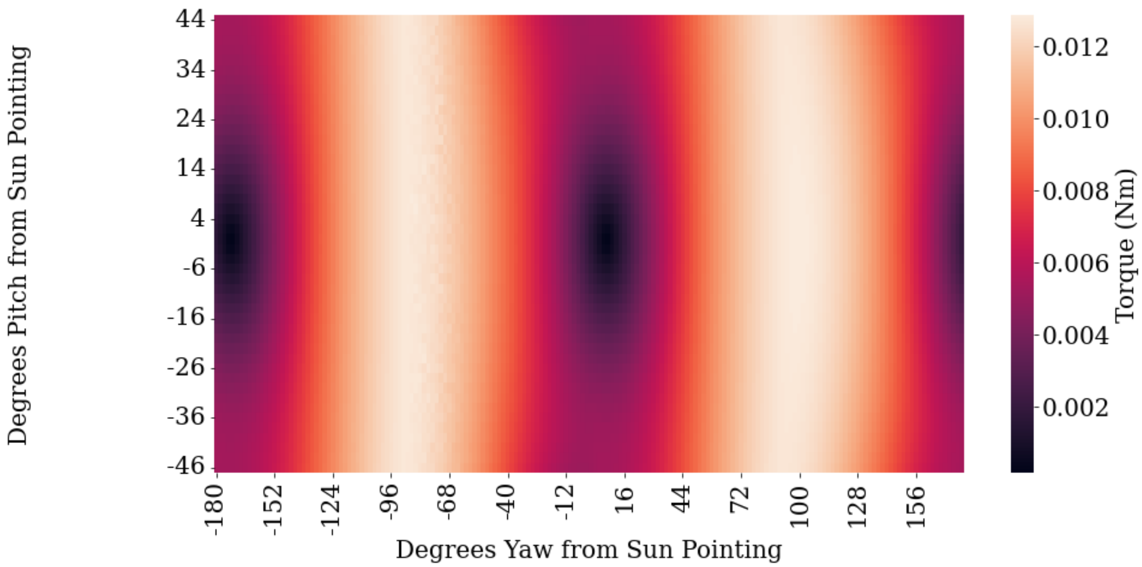

Figure 11: SRP torque magnitude (Nm) for yaw and pitch angle from direct Sun pointing attitude.

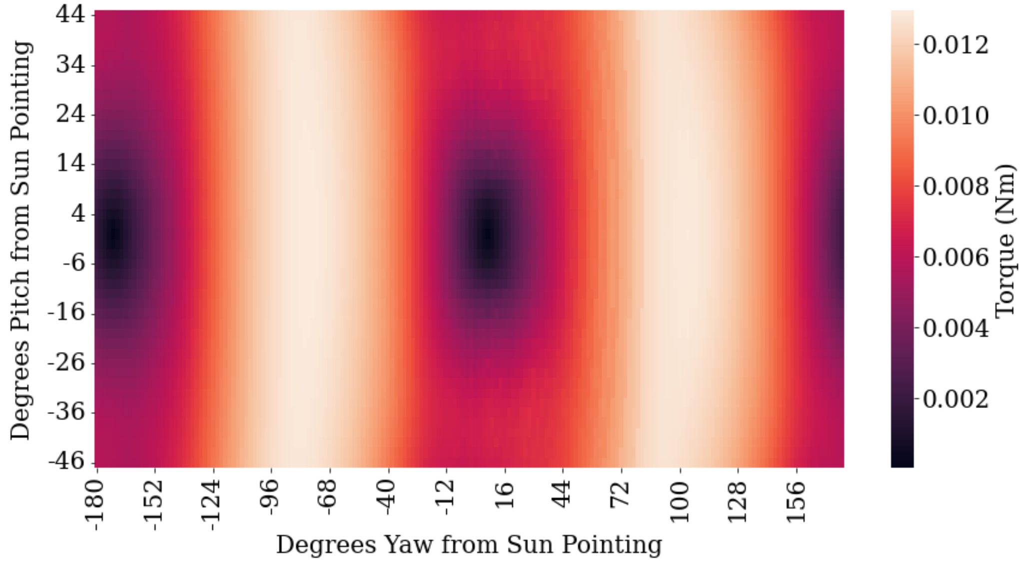

Figure 12: SRP torque magnitude (Nm) for yaw and pitch angle from direct Sun pointing attitude with self shadowing considered.

in approximately 11.5 hours. The lowest SRP torque experienced is near-zero, which could be held indefinitely if not for gravity gradient torques. Below in Figure 12, a similar heatmap is displayed, this time with self-shadowing considered in the torque magnitude calculations.

The difference between these two models are not immediately apparent in this view, so a third heat map is built which is the difference of the flat plate model SRP torque heat map without and with self-shadowing considered. In Figure 13, the SRP torque magnitude error is shown between the flat plate model without and with self-shadowing for solar-oriented attitudes defined by pitch and yaw relative to Sun-pointing.

In this view, it can be seen which attitudes are more sensitive to self-shadowing error than others. There are two distinct "lobes" of SRP error with positive and negative pitching from a minimal yaw angle. These are due to mismodeled shadows cast on the solar panels. Additionally there is a bright and dark vertical area that suggest sensitivity to yaw angles below $\pm$ 70°. This is due to self-shadowing of the Gateway X-axis aligned elements on radially docked elements. There is another band of yaw angles with negative error, and finally the range of yaws where the Gateway structure is "behind" the main solar panels as viewed by the Sun exhibits minimal torque error. The maximum torque error between the models is above 0.0015 Nm−that value of torque would saturate a 250 Nms system in about 1.9 days.

In a similar fashion, this analysis is repeated for the most massive uncrewed configuration in the notional timeline. This configuration has a baseline mass of 97,000 kg and is depicted below in Figure 14. This configuration has two radial components and a human lander system on the Gateway X axis. The center of mass is further from the main solar panels, which creates a longer moment arm for SRP torques.

Below in Figure 15, the torque magnitude error between the native flat plate model and the plate model with self-shadowing considered is shown in a heatmap. In this case the largest errors are within two lobes of low yaw angle and moderate pitch angle, which rise just above 0.003 Nms. For context, that will saturate a 250 Nms RWA system in 23 hours.

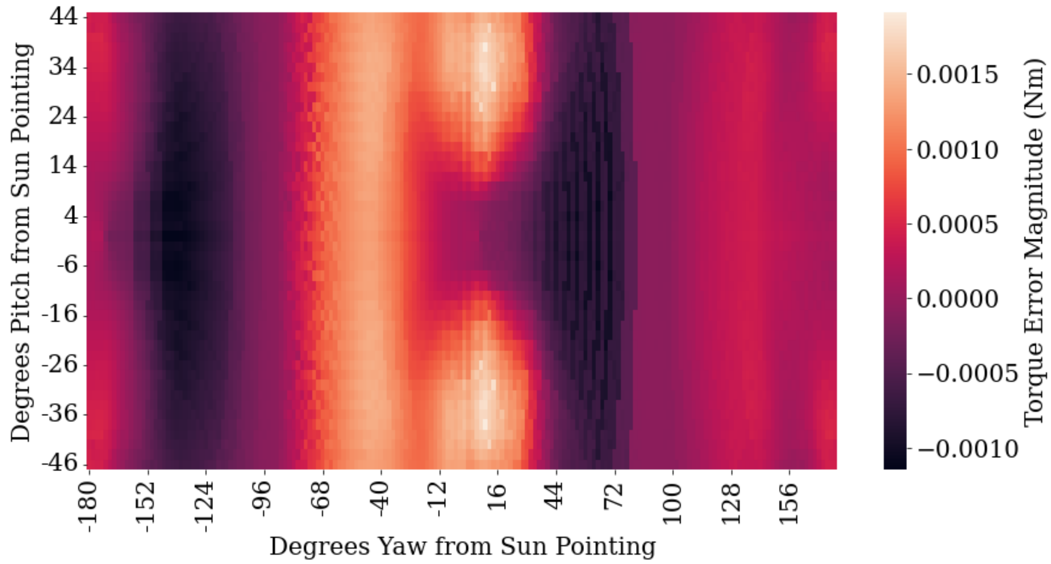

Figure 13: SRP torque magnitude (Nm) error between the flat plate model without and with self-shadowing considered.

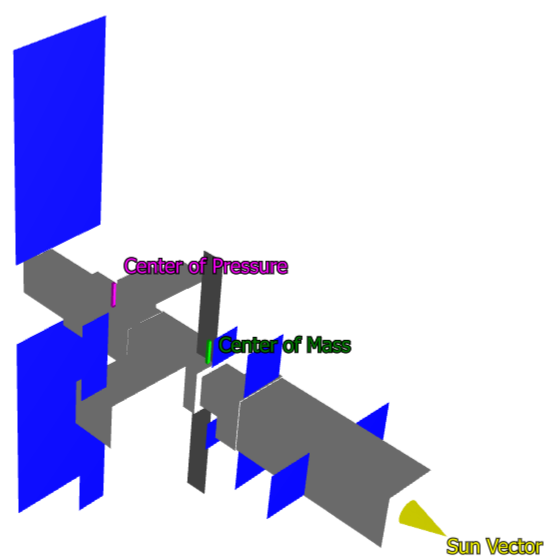

Figure 14: Flat plate model of the largest uncrewed configuration.

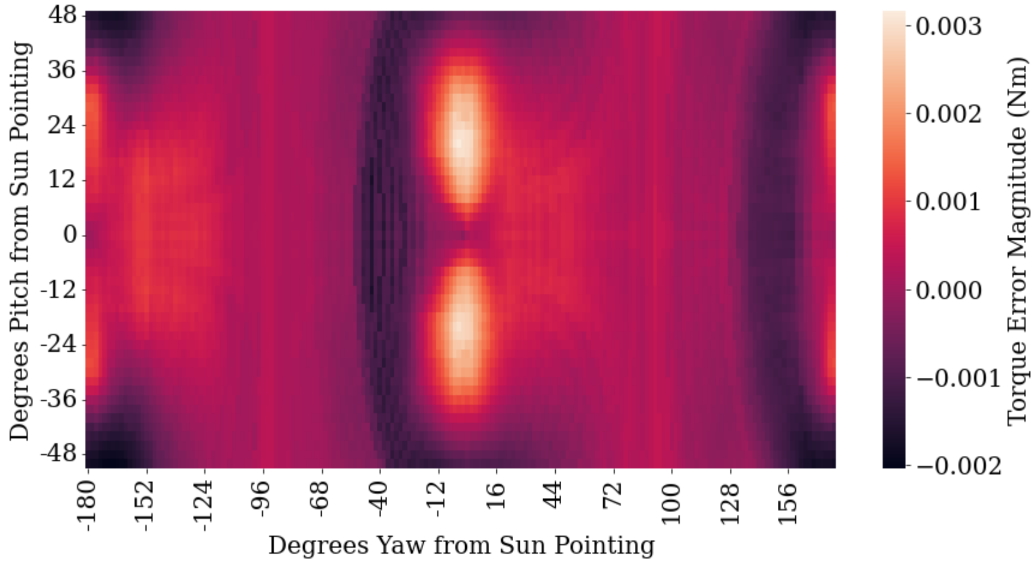

Figure 15: SRP torque magnitude (Nm) error between the flat plate model without and with self-shadowing considered.

The generation of the heatmaps with self-shadowing SRP torque modeling is considerably more taxing computationally than the native flat plates model and is not suited for calculation in-simulation. It depends on mission requirements if the SRP modeling errors calculated above are acceptable for the application. With a constrained attitude set it may be possible to pre-process SRP torques for simulated attitudes that are then applied in-simulation via interpolation. Constraining the attitude set to solar-oriented attitudes that vary only in pitch and yaw is one candidate.

CONCLUSION AND FORWARD WORK

In order to better understand the impact of SRP model fidelity in NRHO operations, a number of analyses are executed to compare SRP flat plate models against spherical models and a slightly more advanced flat plate model with self-shadowing. First, direct propagation comparisons of a flat plate model in the NRHO is compared to different SRP modeling of the Gateway, as well as the same flat plate model but with different values of attitude error. It was found that it is possible for a spherical model to predict well against a flat plate model truth, but the prediction error rises with area error more quickly than a flat plate model with small attitude error. A spherical model with area equal to the flat plate model does not predict well against that flat plate model. It was additionally found that propagating the spherical model is approximately 300% faster than the flat plate model, which creates a tradeoff between accuracy and computational speed.

The next analysis investigated SRP flat plate models within the OD process. An OD simulation was executed wherein the truth spacecraft's SRP model uses flat plates, but the estimated spacecraft uses a spherical model. The simulation in the NRHO used periodic DSN tracking and consistently estimated a C_R with a similar bias that suggested the SRP area as modeled with a sphere is observable in the NRHO. Conversely, the OD simulation was run with ideal initial information of C_R but error on the truth SRP area, and the filter was able to estimate the unique, perturbed SRP area.

The SRP area estimate that the OD filter converged on was then placed onto a spherical SRP model and submitted to a similar prediction test as earlier. It was found that the spherical model with SRP area equal to the estimated value converged upon by the filter predicts as well as a flat plate model with up to ten degrees of attitude error. There may be other operations considerations which would drive the estimated spacecraft to necessitate a flat plate model, such as antenna blocking and attitude considerations for data tracking.

Finally, the impact of self-shadowing is investigated for calculating SPEA. A SRP torque heat map is generated for a configuration using both the nominal flat plate model, and an adjusted flat plate model that attempts to automatically consider self-shadowing. The heatmaps are differenced to identify which solar-oriented attitudes experience the most torque error when self-shadowing is not considered.

These analyses are executed in hopes to inform operations in the NRHO as it pertains to SRP modeling. Utilizing the flat plate model available in the FreeFlyer astrodynamics simulation suite has advantages over simpler models and allows for more deeply informed analysis. There continue to be analysis topics that require attention in the pre-launch phase of Gateway mission design that can benefit from this capability.

Future development of the flat plate model will include antenna analyses such as blocking, attitude constraint analysis, and attitude determination. Proximity Operations and Docking (RPOD) analysis can be informed by the flat plate model, particularly with shadowing considered. The torque maps created earlier can also be directly utilized in simulation by inserting the mapped torques into the simulation rather than simulating the shadowed flat plate model directly in simulation. The pre-processing of attitudes and their resulting torques could be utilized in simulation to apply the correct torque via lookup, speeding up simulation process time while maintaining accuracy of self-shadowed flat plate models.

ACKNOWLEDGEMENTS

The authors would like to thank a.i. solutions, Inc. for partially funding this analysis and presentation that serves to assist Gateway mission design. This work was completed through contract # NNJ13HA01C.

REFERENCES

[1] W. H. Gerstenmaier, "Progress in Defining the Deep Space Gateway and Transport Plan," `https://www.nasa.gov/sites/default/files/atoms/files/nss_chart_v23.pdf`, Mar. 28, 2017.

[2] R. Whitley and R. Martinez, "Options for Staging Orbits in Cis-Lunar Space," *2016 IEEE Aerospace Conference*, 2016.

[3] E. M. Zimovan-Spreen and K. C. Howell, "Dynamical Structures Nearby NRHOs with Applications in Cislunar Space," *2019 AAS/AIAA Astrodynamics Specialist Conference*, Portland, Maine, August 11 – 15, 2019.

[4] D. C. Davis, S. A. Bhatt, K. C. Howell, J. Jang, R. L. Whitley, F. D. Clark, D. Guzzetti, E. M. Zimovan, and G. H. Barton, "Orbit Maintenance and Navigation of Human Spacecraft at Cislunar Near Rectilinear Halo Orbits,"

[5] C. Ott, M. Bollinger, M. Thompson, and N. P. Re, "Range Biases, Measurement Noise, and Perilune Accuracy in Near Rectilinear Halo Orbit Navigation," *AIAA Scitech Forum and Exposition*, San Diego, California, January 2022.

[6] F. L. Markley and J. L. Crassidis, *Fundamentals of Spacecraft Attitude Determination And Control*. New York, NY: Springer, 2014.

[7] A. Nicholson, S. Slojkowski, A. Long, M. Beckman, and R. Lamb, "NASA GSFC Lunar Reconnaissance Orbiter (LRO) Orbit Estimation and Prediction," *SpaceOps 2010 Conference*, Huntsville, Alabama, April 2010.

[8] T. You, A. Halsell, D. Highsmith, M. Jah, S. Demcak, E. Higa, S. Long, and S. Bhaskaran, "Mars Reconnaissance Orbiter Navigation," *AIAA/AAS Astrodynamics Specialists Conference and Exhibit*, Providence, Rhode Island, August 2004.

[9] C. P. Newman, J. R. Hollister, F. S. Miguel, D. C. Davis, and D. J. Sweeney, "Attitude Control and Perturbation Analysis of a Crewed Spacecraft with a Lunar Lander in Near Rectilinear Halo Orbits," *AAS Guidance, Navigation, and Control Conference*, Breckenridge, Colorado, February 2020.

[10] C. P. Newman, D. C. Davis, R. J. Whitley, J. R. Guinn, and M. S. Ryne, "Stationkeeping, Orbit Determination, and Attitude Control for Spacecraft in Near Rectilinear Halo Orbits," *Paper No. AAS 18-388, AAS Astrodynamics Specialist Conference, Snowbird, Utah*, August 2018.